RESEARCH PAPER

Biogenic Silver Nanoparticles from Bruguiera Gymnorhiza: Synthesis, Characterization and Evaluation of Antibacterial, Antioxidant, and Antidiabetic Activities

Anitha Katta[1], Suseela Lanka[1]*

[1] Department of Biosciences and Biotechnology, Krishna University, Machilipatnam-521004, Andhra Pradesh, India.

Corresponding Author: Suseela Lanka, Email: susheelalankaku@gmail.com

Received: *20th Feb, 2026;* ***Revised:*** *4th Mar, 2026;* ***Accepted:*** *25th Mar, 2026;* ***Available Online:*** *10th Apr, 2026*

Abstract

Silver nanoparticles (AgNPs) have recently gained significant attention in the medical field due to their diverse biological properties. The present study aimed to green-synthesis and characterize AgNPs using the aqueous leaf extract of *Bruguiera gymnorhiza*. In addition, the in vitro antibacterial, antioxidant, and antidiabetic activities of both the plant extract and its synthesized AgNPs were evaluated. The powdered leaves were extracted to obtain an aqueous extract, which served as a reducing and stabilizing agent for the synthesis of AgNPs using silver nitrate.

The synthesized nanoparticles were characterized using UV–Visible spectroscopy, Fourier-transform infrared spectroscopy (FTIR), scanning electron microscopy with energy-dispersive X-ray analysis (SEM–EDX), transmission electron microscopy (TEM), and X-ray diffraction (XRD). All experiments were conducted in triplicate (n = 3), and results are expressed as mean ± standard deviation. The UV–Visible spectrum exhibited a surface plasmon resonance (SPR) peak at 424 nm, confirming AgNP formation. FTIR analysis indicated the involvement of functional groups such as C=O, C–H, and O–H in the reduction and capping processes. SEM and TEM analyses revealed predominantly spherical nanoparticles, with sizes ranging from 10 to 50 nm and an average size of 17 nm. EDX analysis showed a characteristic silver peak at 3 keV, while XRD confirmed the crystalline nature of the nanoparticles.

Biological activity assays demonstrated that the synthesized AgNPs exhibited significantly enhanced antibacterial, antioxidant, and antidiabetic activities compared to the crude plant extract. Overall, the findings suggest that *B. gymnorhiza*-mediated AgNPs possess promising therapeutic potential. Further studies are warranted to elucidate their underlying mechanisms and validate their efficacy through in vivo models.

Keywords: *Bruguiera gymnorhiza*, aqueous leaf extract, green synthesis, silver nanoparticles, characterization, antibacterial activity, antioxidant activity, and antidiabetic activity.

How To Cite This Article: Katta A, Lanka S. Biogenic Silver Nanoparticles from Bruguiera Gymnorhiza: Synthesis, Characterization, and Evaluation of Antibacterial, Antioxidant, and Antidiabetic Activities. Int J Drug Deliv Technol. 2026;16(4):388-412. Doi: 10.25258/ijddt.16.4.39

INTRODUCTION

Nanotechnology has become a transformative field in science, providing innovative solutions in medicine, agriculture, and environmental sustainability. Among various nanomaterials, silver nanoparticles (AgNPs) have gained significant attention due to their exceptional physicochemical properties and broad biological activities, including antimicrobial, antioxidant, and other effects[1,2]. Traditionally, chemical and physical methods have been used to produce nanoparticles; however, these approaches often involve toxic reagents, high energy use, and environmental risks. Green synthesis, which utilizes plant extracts, microorganisms, or other biological systems, has gained prominence as an eco-friendly, non-toxic, cost-effective, and sustainable alternative, aligning with principles of green chemistry. Plant-mediated

synthesis, in particular, leverages phytochemicals such as flavonoids, tannins, alkaloids, and phenolic compounds that act as reducing and stabilizing agents, thereby eliminating the need for harmful chemicals[3,4].

The mangrove *Bruguiera gymnorhiza*, belonging to the family Rhizophoraceae, is commonly known as the black mangrove. This species is widely distributed in the Machilipatnam coastal ecosystems and is rich in bioactive compounds with medicinal and ecological significance. The plant extract is known for its rich phytochemical composition, crucial for generating silver nanoparticles. Its phytoconstituents provide a natural platform for reducing silver ions to nanoparticles while simultaneously capping and stabilizing them[5,6]. The green synthesis method leverages the inherent reducing capabilities of biomolecules present in the plant extract, such as flavonoids and terpenoids, to reduce silver ions into metallic silver nanoparticles[7]. The biogenic reduction not only circumvents the need for hazardous chemical reducing agents but also yields nanoparticles with distinct surface properties that can enhance their stability and biological efficacy[8-10]. This environmentally benign approach aligns with green chemistry principles, offering a cost-effective and scalable alternative to conventional physical and chemical synthesis routes[11,12]. The use of plant material-assisted synthesis for AgNPs, incorporating unpurified plant extracts, contributes to the complexity and diversity in their behavior, selectivity, and sensitivity, which can be leveraged for advanced applications[13]. This approach not only significantly reduces manufacturing costs but also reduces energy consumption compared to traditional methods[14]. Furthermore, green synthesis methods, besides their cost-effectiveness and scalability, mitigate the environmental and health risks associated with conventional chemical reduction methods[15,16]. The biogenic production of AgNPs has garnered significant interest within the scientific community, particularly due to its inherent simplicity, environmental consciousness, and the elimination of toxic and expensive chemicals[17,18]. Such plant-mediated synthesis methods are increasingly recognized for their ability to produce nanoparticles with enhanced size uniformity and stability, alongside intriguing pharmacological properties attributable to their biocompatibility and nano-dimension[19]. These eco-friendly synthesis methods also overcome the limitations of physical and chemical approaches, which often involve high energy requirements, high fabrication costs, and the generation of toxic byproducts[20]. The use of mangrove plants not only highlights the potential of underexplored biodiversity but also aligns with sustainable resource utilization.

The synthesized silver nanoparticles were characterized using various analytical techniques to confirm their successful formation. UV–Visible spectroscopy was used to monitor surface plasmon resonance, while Fourier-transform infrared spectroscopy (FTIR) identified functional groups involved in reduction and stabilization. Morphological features were examined using Scanning Electron Microscopy (SEM) coupled with Energy Dispersive X-ray (EDX) for elemental analysis. Transmission Electron Microscopy (TEM) is commonly used to determine particle size and shape, and X-ray Diffraction (XRD) provides information on crystalline structure. These techniques collectively help in confirming the size, shape, composition, crystallinity, and stabilization of the synthesized nanoparticles.

In addition to synthesis and characterization, the evaluation of the biological activities of *Bruguiera gymnorhiza*-mediated silver nanoparticles is of considerable interest. Plant-derived silver nanoparticles have been widely reported to exhibit significant antibacterial activity against both Gram-positive and Gram-negative bacteria, including *Staphylococcus aureus* and *Escherichia coli*, attributed to the synergistic effects of silver and plant-derived bioactive compounds[21]. Furthermore, their antioxidant potential can be assessed using in vitro assays such as DPPH radical scavenging, ferric reducing antioxidant power (FRAP), and nitric oxide scavenging, which reflect the ability to neutralize reactive species[22]. In addition, the antidiabetic potential of such nanoparticles is commonly evaluated through α-amylase and α-glucosidase inhibition assays, along with glucose uptake studies, indicating their possible role in glycemic control[23].

The present study aims to synthesize and characterize silver nanoparticles using the aqueous leaf extract of *Bruguiera gymnorhiza* and to evaluate their antibacterial, antioxidant, and antidiabetic activities. Previous studies have reported that *B. gymnorhiza* is rich in diverse bioactive compounds, including terpenoids, flavonoids, alkaloids, phenolics, and quinones, which are associated with various pharmacological properties. These phytoconstituents are known to contribute to significant biological activities such as antimicrobial, antioxidant, and antidiabetic effects. Therefore, the green synthesis of silver nanoparticles using *B. gymnorhiza* offers a

promising, eco-friendly approach for the development of biologically active nanomaterials. This work highlights the potential of mangrove-derived resources in advancing sustainable nanotechnology and biomedical applications.

MATERIALS AND METHODS

Collection of samples and preparation of plant extract

The fresh leaves of *Bruguiera gymnorrhiza* were collected from the Pedapatnam of the Machilipatnam coastal regions of Andhra Pradesh (Figure 1). The plant genus and the species were confirmed by the Department of Biosciences and Biotechnology, Krishna University, Machilipatnam, Andhra Pradesh, India. The collected leaves were washed in running water to remove dust and other impurities, followed by rinsing with double-distilled water and shade-dried at room temperature for 10-15 days. The fully dried leaves were powdered with a sterile electric blender. The powdered samples were preserved in an airtight container and away from the sunlight for further use. For the preparation of the aqueous extract, 10 grams of leaf powder was mixed with 1000 ml of double-distilled water in a beaker, followed by heating at 65°C for 30 minutes with a magnetic hot plate stirrer. This was then cooled and filtered by Whatman No. 1 filter paper. The obtained extract was stored at 4°C for further experiments.

Figure 1: *Bruguiera gymnorrhiza* from the Pedapatnam of the Machilipatnam coastal region

Phytochemical analysis

The crude aqueous leaf extract of *Bruguiera gymnorrhiza* was assessed for the presence of various groups of metabolites, including glycosides, alkaloids, reducing sugars, carbohydrates, proteins, flavonoids, phenolic compounds, amino acids, tannins, terpenoids, saponins, phytosterols, triterpenoids, diterpenes, quinones, and anthraquinones, using standard procedures[24].

Synthesis of Silver Nanoparticles

A total of 10 mL of *Bruguiera gymnorrhiza* leaf extract was added to 90 mL of 1 mM aqueous $AgNO_3$ solution (1:9 ratio) in a beaker and subjected to vigorous mixing for 30 s using a magnetic hot plate stirrer maintained at 80 °C. The reaction mixture was incubated in the dark at room temperature (26–27 °C) to minimize unwanted photochemical reactions. The formation of silver nanoparticles was initially indicated by a visible colour change of the reaction mixture from colourless to brown, confirming the reduction of Ag^+ ions.

Following complete reaction, the colloidal suspension containing AgNPs was centrifuged at 10,000 rpm for 10 min. The obtained pellet was washed and redispersed in double-distilled water to remove residual plant biomolecules and unreacted constituents. This purification step was repeated as necessary. The purified nanoparticles were then dried to obtain a fine powder for further characterization and analysis.

Characterization of Synthesized Silver Nanoparticles

All the characterizations performed in this investigation used a single batch of the synthesized *Bruguiera gymnorhiza* AgNPs. An array of analytical methods was employed to characterize the produced AgNPs and these included UV–Vis, FTIR, SEM, EDX, TEM and XRD.

UV–Visible Spectroscopy Analysis

To confirm the reduction of silver ions and the formation of colloidal silver nanoparticles, UV–visible spectroscopy was performed using a Shimadzu UV-1900 spectrophotometer. An aliquot of 1 mL of the reaction mixture was placed in a quartz cuvette, and the absorption spectrum was recorded over a wavelength range of 200–800 nm. Distilled water was used as the control, while a 1 mM $AgNO_3$ solution served as the blank. The characteristic surface plasmon resonance (SPR) peak of silver nanoparticles was monitored to confirm their formation.

Fourier Transform Infrared Spectroscopy (FTIR) Analysis

Fourier Transform Infrared (FTIR) spectroscopy was performed to identify the functional groups involved in the reduction and stabilization of silver nanoparticles. The analysis was carried out using an FT/IR-4700 Type A spectrophotometer. The nanoparticle sample was prepared by centrifuging the colloidal suspension at 10,000 rpm for 15 min, followed by drying to obtain a fine powder. The dried AgNP sample was then subjected to FTIR analysis in the transmission mode over a spectral range of 4000–400 cm^{-1} with a resolution of 4 cm^{-1}. The obtained spectra were used to determine the biomolecular functional groups responsible for the reduction of silver ions and capping of the nanoparticles.

Scanning Electron Microscopy (SEM) and Energy Dispersive X-ray (EDX) Analysis

The surface morphology and elemental composition of the synthesized silver nanoparticles were analyzed using scanning electron microscopy (SEM) coupled with Energy Dispersive X-ray (EDX) spectroscopy (TESCAN VEGA 3 / TESCAN MIRA LMS).

For SEM analysis, the nanoparticle sample was dispersed in distilled water and subjected to sonication for 5–10 min to achieve uniform dispersion. A drop of the suspension was placed onto a carbon-coated grid/stub and allowed to air-dry completely under ambient conditions. The dried sample was examined under SEM at an accelerating voltage of 15–20 kV with suitable magnifications ranging from ×10,000 to ×100,000 to evaluate the morphology, size, and surface characteristics of the nanoparticles.

For EDX analysis, the purified AgNPs were deposited onto a carbon-coated copper grid and dried thoroughly. The sample was then subjected to EDX analysis at an accelerating voltage of 15–20 kV, and the obtained spectra were used to determine and confirm the elemental composition of the synthesized nanoparticles.

Transmission Electron Microscopy (TEM)

The synthesized silver nanoparticles' particular size, shape, and crystalline features were visualized by using a TEM (Talos L120C) manufactured by Thermo Fisher Scientific. One aliquot of the silver nanoparticle dispersion was carefully mounted on a carbon-coated copper grid and dried naturally under laboratory conditions before analysis. Then, imaging was performed at an accelerating voltage of 120 kV. The acquired Transmission electron microscopy micrographs enabled direct assessment of nanoparticle shape and size distribution, revealing predominantly spherical particles, and the crystalline nature of the silver nanoparticles was verified using selected area electron diffraction patterns.

X-ray Diffraction (XRD) Analysis

The crystalline structure, phase purity, and average crystallite size of the synthesized silver nanoparticles were determined using X-ray diffraction (XRD) analysis. The measurements were carried out on a Bruker D8 Advance X-ray diffractometer (USA) equipped with Cu-Kα radiation (λ = 1.5406 Å).

The dried nanoparticle powder was uniformly mounted onto the sample holder and scanned over a 2θ range of 20°–80° at a scanning rate of 2° min^{-1} under an operating voltage of 40 kV and a current of 30 mA. The obtained diffraction patterns were analyzed to identify the characteristic Bragg reflections corresponding to the face-centered cubic (fcc) structure of metallic silver.

Biological Activities of Synthesized Silver Nanoparticles

Antimicrobial Activity

The test microorganisms used for antibacterial sensitivity testing included two gram-positive and two gram-negative organisms. *Bacillus subtilis* and *Staphylococcus aureus* were used as model Gram-positive bacteria, and *Pseudomonas aeruginosa* and *Escherichia coli* were used as model Gram-negative bacteria. All cultures used are pure and obtained from a standard organisation like the National Collection of Industrial Microorganisms (NCIM), Pune, India. All strains were maintained on Nutrient agar at 4°C, and the bacterial strains were subcultured on nutrient agar slants for 24 h before being used for antibacterial assays.

Antibacterial activity

Disc Diffusion Method

The antibacterial efficacy of the synthesized silver nanoparticles using *Bruguiera gymnorrhiza* aqueous leaf extract was evaluated by the disc diffusion method. The bacterial strains were cultured on nutrient agar (HiMedia) slants and incubated at 37 °C for 24 h. A loopful of each culture was inoculated into nutrient

agar medium, which was then poured into Petri plates using the pour plate technique and allowed to solidify.

Commercial antibiotic susceptibility discs (HiMedia), including tetracycline (30 mcg), erythromycin (15 mcg), ciprofloxacin (5 mcg), vancomycin (30 mcg), nitrofurantoin (300 mcg), and azithromycin (15 mcg), were used. The discs were incubated with the silver nanoparticle sample, and the impregnated discs were placed onto the surface of nutrient agar plates inoculated with the selected test organisms. Along with these, discs containing only silver nanoparticles and antibiotic discs alone (positive control) were also included.

The plates were incubated at 37 °C for 24 h in an upright position and subsequently observed for the formation of zones of inhibition. The diameter of the inhibition zones was measured in millimeters (mm) to assess antimicrobial activity. All experiments were conducted in triplicate.

Antioxidant Activity

The antioxidant capacity of *Bruguiera gymnorhiza* derived silver nanoparticles (AgNPs) and their aqueous leaf extract was determined using three in vitro spectrophotometric assays: DPPH (2,2-Diphenyl-1-picrylhydrazyl) radical scavenging, Ferric Reducing Antioxidant Power (FRAP), and Nitric Oxide (NO) scavenging. These assays assess the ability of samples to neutralize reactive oxygen and nitrogen species, which are known to cause oxidative damage to biomolecules[22]. Together, these complementary tests provide a broad evaluation of the radical-scavenging and reducing efficiency of the synthesized AgNPs compared with the crude *Bruguiera* extract[25].

DPPH Assay for *Bruguiera gymnorhiza*–Derived Silver Nanoparticles

The DPPH assay estimates free-radical quenching through electron or hydrogen donation. The antioxidant activity of silver nanoparticles (AgNPs) synthesized using aqueous *Bruguiera gymnorhiza* leaf extract was evaluated by the DPPH (2,2-diphenyl-1-picrylhydrazyl) radical-scavenging assay, following the general procedure described by Gulçin and Alwasel (2023)[22], with modifications for nanoparticle systems. A fresh 0.004% (w/v) DPPH solution was prepared in ethanol and protected from light. The AgNP stock dispersions were prepared, and the *Bruguiera* aqueous extract was diluted in the same solvent system to obtain working concentrations of 10, 25, 50, 75 and 100 µg mL^{-1}, expressed as silver or dry-mass equivalent. Ascorbic acid was used as a positive control.

For each test, 1.0 mL of sample (AgNP or extract) was mixed with 2.0 mL of DPPH solution and incubated in the dark at room temperature for 30 minutes. All measurements were performed in triplicate to ensure reproducibility. Because biologically synthesized AgNPs typically exhibit a surface plasmon resonance (SPR) band in the 380–450 nm range, which may cause baseline interference, a nanoparticle blank (A_{NB}) consisting of 1.0 mL sample + 2.0 mL solvent (no DPPH) was included for each concentration and subtracted from the test reading. A DPPH control ($A_{control}$) (2.0 mL DPPH + 1.0 mL solvent) and a solvent blank were also prepared.

Absorbance was recorded at 517 nm using a UV–Vis spectrophotometer (Shimadzu UV-1800). The percentage of radical-scavenging activity was calculated using the following formula[26] :

$$\text{DPPH scavenging activity (\%)} = \frac{A_{\text{control}} - (A_{\text{test}} - A_{NB})}{A_{\text{control}}} \times 100$$

Where,

$A_{control}$ = Absorbance of DPPH solution without sample (represents 100% free radicals),

A_{test} = Absorbance of DPPH solution with AgNP or extract

A_{NB} = Absorbance of nanoparticle blank (without DPPH).

Dose–response curves were plotted between percent inhibition and concentration, and IC_{50} values were calculated as the concentration required to scavenge 50% of DPPH radicals, expressed as mean ± SD (n = 3).

FRAP Assay for *Bruguiera gymnorhiza*–Derived Silver Nanoparticles

The FRAP method measures the reducing power of antioxidants by converting ferric ions to ferrous ions. The ferric reducing antioxidant power (FRAP) of silver nanoparticles (AgNPs) synthesized using aqueous *Bruguiera gymnorhiza* leaf extract was evaluated according to the method originally described by Benzie and Strain (1996)[27] and modified by Banerjee et al. (2008)[28], with additional precautions to correct for nanoparticle optical interference.

Briefly, 1.0 mL of each test sample, *Bruguiera gymnorhiza*-derived AgNP dispersion or the *Bruguiera gymnorhiza* aqueous extract, was mixed with 1.0 mL of

0.2 M sodium phosphate buffer (pH 6.6) and 1.0 mL of 1% (w/v) potassium ferricyanide in separate test tubes. The mixtures were incubated at 50 °C for 20 minutes in a temperature-controlled water bath to promote the reduction of ferricyanide to ferrocyanide. After incubation, 1.0 mL of 10% (w/v) trichloroacetic acid (TCA) was added to each tube to stop the reaction. The tubes were centrifuged at 3,000 rpm for 10 minutes at room temperature to obtain clear supernatants. An aliquot of 1.0 mL of each supernatant was transferred into a fresh tube containing 1.0 mL of deionized water and 200 µL of 0.1% (w/v) ferric chloride ($FeCl_3$). After 5 minutes of incubation at room temperature, the absorbance of the resulting Prussian blue complex was recorded at 700 nm using a UV–Vis spectrophotometer (Shimadzu UV-1800).

A nanoparticle blank (A_{NB}) (1.0 mL of AgNP dispersion treated identically but without potassium ferricyanide) was included for each concentration to correct for baseline interference caused by AgNPs. Ascorbic acid (10–100 µg·mL⁻¹) was used as a positive control. All measurements were performed in triplicate (n = 3) and expressed as mean ± SD. The ferric reducing antioxidant power was expressed as the increase in absorbance at 700 nm after blank subtraction, calculated as follows:

$$\Delta A_{700} = (A_{700}(\text{sample}) - A_{\text{blank}}) - A_{NB}$$

Where,

$\boldsymbol{\Delta A_{700}}(\text{sample})$= Absorbance of the reaction mixture containing AgNPs or extract measured at 700 nm.

$\mathbf{A_{blank}}$ = Absorbance of the blank

$\mathbf{A_{NB}}$ = Absorbance of nanoparticle blank (without potassium ferricyanide).

Nitric Oxide (NO) Scavenging Assay for *Bruguiera gymnorhiza*–Derived Silver Nanoparticles

The NO scavenging assay evaluates inhibition of nitric oxide formation using the Griess reagent. The nitric oxide (NO) radical-scavenging activity of silver nanoparticles (AgNPs) synthesized using aqueous *Bruguiera gymnorhiza* leaf extract was determined using the sodium nitroprusside (SNP) method, with modifications to account for nanoparticle interference.

In this assay, 10 mM sodium nitroprusside (SNP) in phosphate-buffered saline (PBS, pH 7.4) was used as the source of nitric oxide. Various concentrations of *Bruguiera*-derived AgNP dispersions and the aqueous leaf extract (10, 25, 50, 75, and 100 µg mL⁻¹) were prepared in deionized water. For each reaction, 1.0 mL of sample was mixed with 2.0 mL of SNP solution and incubated under light at room temperature for 150 minutes to facilitate nitric oxide generation. After incubation, 0.5 mL of the reaction mixture was combined with 1.0 mL of freshly prepared Griess reagent (1% sulfanilamide in 5% phosphoric acid and 0.1% naphthyl ethylenediamine dihydrochloride), mixed well, and allowed to stand for 5 minutes for color development[29].

The absorbance of the resulting pink chromophore was measured at 540 nm using a UV-Visible spectrophotometer (Shimadzu UV-1800) against the reagent blank. A nanoparticle blank (A_{NB}) (1.0 mL AgNP dispersion + 2.0 mL PBS, no SNP) was included for each concentration to correct for background absorbance or direct reaction of nanoparticles with the Griess reagent. Ascorbic acid (10–100 µg·mL⁻¹) served as a positive control.

Nitric oxide scavenging activity was calculated using the following formula:

$$\text{NO Scavenging Activity (\%)} = \frac{A_{\text{control}} - (A_{\text{test}} - A_{NB})}{A_{\text{control}}} \times 100$$

Where,

$\mathbf{A_{control}}$ = Absorbance of SNP + Griess reagent (without sample, representing 100% NO generation), $\mathbf{A_{test}}$ = Absorbance of the reaction mixture containing AgNPs or extract, and $\mathbf{A_{NB}}$ = Absorbance of nanoparticle blank (no SNP).

The percentage inhibition was plotted against concentration to obtain IC_{50} values (the concentration required to scavenge 50% of NO radicals). All experiments were performed in triplicate and expressed as mean ± SD (n = 3).

Anti-Diabetic Activity

Diabetes mellitus is a metabolic disorder characterized by sustained hyperglycemia caused by impaired insulin secretion, defective insulin action, or a combination of both, resulting in disturbances in carbohydrate, lipid, and protein metabolism[26]. In recent years, plant-mediated silver nanoparticles have gained considerable interest owing to their enhanced biological activity, environmentally friendly synthesis, and improved biocompatibility. In the present investigation, the anti-diabetic potential of silver nanoparticles synthesized using *Bruguiera gymnorhiza* was assessed through

three in vitro experimental models, namely α-amylase inhibition, α-glucosidase inhibition, and glucose uptake by yeast cells assay.

Assay of α-Amylase Inhibition Activity

The inhibitory effect of *Bruguiera gymnorhiza*–derived silver nanoparticles (AgNPs) on α-amylase activity was evaluated using the starch DNSA colorimetric method as described by Ali et al. (2006)[30]. A 1% (w/v) starch solution was prepared by dissolving 1 g of soluble starch in 100 mL of 20 mM phosphate buffer (pH 6.9) containing 6.7 mM sodium chloride. Porcine pancreatic α-amylase (27.5 mg) was dissolved in 100 mL of the same buffer to prepare the enzyme solution.

To 100 µL of AgNP suspension at varying concentrations (2, 4, 8, 10, and 15 µg/mL), 200 µL of α-amylase solution was added, and the mixture was incubated at 37 °C for 20 minutes. Subsequently, 100 µL of 1% starch solution was added, followed by further incubation at 37 °C for 10 minutes. The enzymatic reaction was terminated by the addition of 200 µL of DNSA reagent, prepared by dissolving 1 g of 3,5-dinitrosalicylic acid, 30 g of sodium potassium tartrate, and 20 mL of 2 N sodium hydroxide, with the final volume adjusted to 100 mL using distilled water. The reaction mixture was then heated in a boiling water bath for 5 minutes. After cooling, the mixture was diluted with 2.2 mL of distilled water, and the absorbance was measured at 540 nm using a UV–Visible spectrophotometer (Shimadzu UV-1800). Blank samples were prepared by replacing the enzyme solution with distilled water, while the control contained all reagents except AgNPs and represented 100% enzyme activity. Acarbose was used as a positive control. All experiments were carried out in triplicate.

$$\% \text{ α-amylase inhibition} = \frac{\text{Abs}_{control} - \text{Abs}_{sample}}{\text{Abs}_{control}} \times 100$$

Assay of α-Glucosidase Inhibition Activity

The α-glucosidase inhibitory activity of *Bruguiera gymnorhiza*–derived AgNPs was determined using a modified method described by Kim et al. (2009)[31]. The α-glucosidase enzyme (1 mg) was dissolved in 100 mL of phosphate buffer (pH 6.8). To 100 µL of AgNP suspension at concentrations of 2, 4, 8, 10, and 15 µg/mL, 200 µL of α-glucosidase solution was added, and incubated at 37 °C for 20 minutes.

The reaction was initiated by adding 100 µL of 3 mM p-nitrophenyl-α-D-glucopyranoside (p-NPG), and incubated at 37 °C for 10 minutes. The reaction was terminated by the addition of 2 mL of 0.1 M sodium carbonate solution. The release of p-nitrophenol was measured spectrophotometrically at 405 nm using a UV-visible spectrophotometer (Shimadzu UV-1800).

Acarbose was employed as the standard inhibitor. The IC_{50} value was defined as the concentration of AgNPs required to inhibit 50% of α-glucosidase activity under the assay conditions. All experiments were performed in triplicate.

$$\% \text{ α-glucosidase inhibition} = \frac{\text{Abs}_{control} - \text{Abs}_{sample}}{\text{Abs}_{control}} \times 100$$

Glucose Uptake by Yeast Cells Method

The glucose uptake–enhancing potential of *Bruguiera gymnorhiza*–derived AgNPs was evaluated using a yeast cell model as described by Gupta et al. (2013)[32]. Commercial baker's yeast was repeatedly washed with distilled water and centrifuged at 3000 g for 5 minutes until a clear supernatant was obtained. A 10% (v/v) yeast suspension was then prepared.

AgNP samples at concentrations ranging from 10 to 50 µg/mL were added to 1 mL of glucose solutions with concentrations of 5, 10, and 20 mM and incubated at 37 °C for 10 minutes. The experiment was initiated by the addition of 100 µL of yeast suspension, followed by vortexing and incubation at 37 °C for 60 minutes. After incubation, the reaction mixtures were centrifuged at 3000 rpm for 5 minutes, and the residual glucose content present in the supernatant was determined spectrophotometrically. Metformin was used as a reference antidiabetic drug. All experiments were carried out in triplicate.

$$\% \text{ Increase in glucose uptake} = \frac{\text{Abs}_{control} - \text{Abs}_{sample}}{\text{Abs}_{control}} \times 100$$

Where,

$\text{Abs}_{(control)}$ represents the absorbance of the control reaction without AgNPs, and

$\text{Abs}_{(sample)}$ represents the absorbance in the presence of *Bruguiera gymnorhiza*–derived AgNPs.

RESULTS AND DISCUSSION

Phytochemical Analysis

The preliminary phytochemical assessment of *Bruguiera gymnorrhiza* leaf extracts revealed the

presence of several bioactive compounds, including carbohydrates, alkaloids, proteins and amino acids, reducing sugars, flavonoids, phenolic compounds, tannins, saponins, phytosterols, diterpenes, and quinones (Table 1). These phytochemicals play a critical role in the green synthesis of silver nanoparticles (AgNPs), acting as both reducing and stabilizing agents. Functional groups such as hydroxyl (–OH) and carbonyl (–C=O) present in flavonoids, phenolics, tannins, and quinones facilitate the reduction of Ag^{+} ions to metallic Ag^{0}, evidenced by the colour change from colourless to brown during synthesis. Meanwhile, proteins, amino acids, saponins, and terpenoids serve as natural capping agents, preventing nanoparticle aggregation and contributing to their stability, controlled size, and uniform morphology. Moreover, these surface-bound phytochemicals can enhance the biological activity of AgNPs, improving antimicrobial, antioxidant, and antidiabetic properties through synergistic effects. The use of plant-derived biomolecules thus enables an eco-friendly, cost-effective, and biocompatible synthesis of AgNPs, highlighting the importance of the phytochemical composition in the formation, stabilization, and functional efficacy of the nanoparticles.

Table 1: Phytochemical analysis of aqueous leaf extract of *Bruguiera gymnorhiza.*

Phytochemicals	Test	Test procedure	Observation	*B. gymnorhiza*
Alkaloids	Dragendorff's Test	In 2 mL of aqueous extract, 1 mL of Dragendorff's reagent was added	Orange-red precipitate	+
Carbohydrates	Barfoed's test	1mL of aqueous extract, 1 mL of Barfoed's reagent was added and heated for 2 min.	Red precipitate	+
	Molish's test	In 2 ml of the aqueous extract, add 2 drops of alcoholic α-naphthol, followed by the addition of conc. H_2SO_4 (along the sides of the test tube)	Formation of a violet ring	+
	Seliwanoff's test	In 1mL aqueous extract, 3 mL Seliwanoff's reagent was added and heated for 1 min.	Red colour	+
	Test of starch	In 2 mL of aqueous extract, add a few mL of iodine solution.	Colour change	+
Reducing sugars	Benedict's test	In 1 mL of aqueous extract, 1 mL of Benedict's reagent was added and boiled for 2 min.	Green/yellow/red colour	++
Glycosides	Modified Borntrager's test	In 1 ml of the plant extract, ferric chloride solution was added and boiled for 5 minutes after cooling, equal volumes of benzene were added, then the benzene layer was separated in an ammonia solution.	Rose-pink to blood red colour	+
	Conc. H_2SO_4 test	In 5ml of aqueous extract, add 2 mL of glacial acetic acid and a drop of 5% $FeCl_3$ followed by the addition of conc. H2SO4.	Brown ring appears	+
Proteins and amino acids	Ninhydrin test	In 2 mL of aqueous extract, add 2 drops of Ninhydrin solution and heat for 2min.	Purple colour	++
	Xanthoproteic test	In 2ml of aqueous extract, add a few drops of conc. Nitric acid.	Yellow colour	++

Flavonoids	Ferric chloride test	In 2 ml of aqueous extract, add a few drops 10% ferric chloride solution	Green precipitate	++
	Ammonia test	In 2ml of aqueous extract, add 5 mL dil. Ammonia solution followed by conc. H_2SO_4	Yellow colour	+
Phenolic compounds	Ferric chloride test	In 2 mL of aqueous extract, add a few drops 5% ferric chloride solution.	Dark green/bluish black colour	++
	Lead acetate test	In 2 mL of aqueous extract, add 3 mL of 10% lead acetate sol.	White precipitate	+
	Ellagic Acid Test	In 2 mL of aqueous extract, add 5% glacial acetic acid, followed by 5% sodium nitrite solution	Solution turns muddy / Niger brown precipitate	-
Tannins	Gelatin test	In 2 mL of aqueous extract, add 1% gelatin solution, followed by 10% NaCl	White precipitate	-
	10% NaOH test	In 2 mL of aqueous extract, add 4mL of 10% NaOH, then shake well	Formation of emulsion	-
	Braymer's test	In 2 mL of aqueous extract, add a few drops 10% Ferric chloride solution	Blue-green colour	+
Saponins	Foam test	In 0.5 g aqueous plant extract, add 2mL of water (vigorously shaken)	Persistent foam for 10 min.	+
	$NaHCO_3$ test	In 2 mL of aqueous extract, add a few mL of sodium bicarbonate solution, followed by distilled water (vigorously shaken)	Stable honeycomb-like froth	+
Phytosterols	Libermann-Burchard's test	In 2 mL of aqueous extract, add 2mL of acetic anhydride followed by 1-2 drops of conc. H_2SO_4 (along the side of the test tube)	An array of colour changes	+
	Hesse's response test	In 2 mL of aqueous extract, add 2mL chloroform followed by 2mL of conc. H_2SO_4	Pink ring / Red colour (in lower chloroform layer)	-
Diterpenes	Copper acetate test	In 2 mL of aqueous extract, add a few drops of copper acetate solution	Emerald green colour	+
Quinones	Sulphuric acid test	In 2 mL of aqueous extract, add isopropyl alcohol followed by a few drops of conc. H_2SO_4	Red colour	+
	Alcoholic KOH test	In 2 mL of aqueous extract, add a few mL of alcoholic potassium hydroxide	Red to blue colour	+

(++) Highly present (+) Present (-) absent

The phytochemical profile observed in the present study, characterized by the presence of tannins, alkaloids, glycosides, flavonoids, and saponins, is largely consistent with earlier reports on *Bruguiera gymnorhiza*. Mangrove species, including *B. gymnorhiza*, are well recognized for their richness in polyphenolic compounds such as flavonoids and tannins, which are associated with diverse pharmacological properties, including antinociceptive and antidiarrheal activities[33]. The detection of these compounds in the current study aligns with the established chemical composition of mangrove flora.

Previous investigations have indicated that *B. gymnorhiza*, being adapted to saline and stress-prone coastal environments, tends to accumulate a high proportion of polar phytoconstituents, particularly in aqueous extracts[34]. This observation supports the present findings, where aqueous extraction yielded a broad spectrum of bioactive compounds.

Comparative studies further reinforce these results. For instance, leaf extracts from *B. gymnorhiza* collected in Kumarakom, Kerala, were reported to contain alkaloids, terpenoids, phenols, and quinones, contributing to significant antimicrobial and antioxidant activities[35]. Similarly, studies conducted on different plant parts from specimens collected in Mauritius demonstrated that methanolic fruit extracts exhibited higher levels of phenolics, tannins, and triterpenoids[36]. While these variations highlight the influence of solvent systems and plant parts on phytochemical composition, the consistent detection of phenolic and alkaloid classes across studies—including the present one—suggests a conserved phytochemical pattern in this species.

Overall, the present findings are in agreement with earlier reports and further substantiate that *B. gymnorhiza* is a rich source of bioactive secondary metabolites. Minor variations in phytochemical profiles among studies may be attributed to differences in geographical location, environmental conditions, and extraction methodologies.

Synthesis of Silver Nanoparticles

The addition of *Bruguiera gymnorrhiza* aqueous leaf extract to a 1 mM $AgNO_3$ solution resulted in a visible colour change from yellowish to brown within 30 min, indicating the bioreduction of silver ions (Ag^+) to silver nanoparticles (Ag^0). After 1 h, the reaction was complete, with the solution exhibiting a stable brown colour, confirming the formation of silver nanoparticles (Fig. 2).

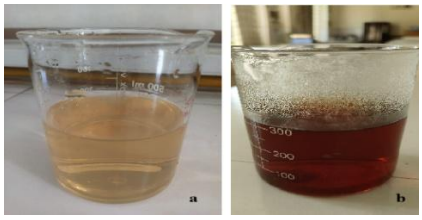

Figure 2. Formation of silver nanoparticles. (a) Addition of *Bruguiera gymnorrhiza* aqueous leaf extract to 1 mM $AgNO_3$ solution. (b) Colour change from yellowish to brown, indicating the bioreduction of Ag^+ ions and formation of silver nanoparticles (AgNPs).

The observations in the present study are in agreement with earlier reports on mangrove-mediated synthesis of silver nanoparticles. A similar visual transition in reaction colour has been documented for *Bruguiera cylindrica* collected from the Pichavaram mangrove forests in Tamil Nadu, where the addition of leaf extract to a colourless silver nitrate solution resulted in a gradual change to yellow and subsequently dark brown, indicating the formation of AgNPs[37]. This characteristic colour change, attributed to surface plasmon resonance, supports the findings of the current study and confirms the reduction of silver ions by plant-derived phytochemicals.

Comparable results have also been reported for AgNPs synthesized using leaf extracts of *Rhizophora stylosa* from the mangrove forests of the Riau Archipelago, Indonesia. These nanoparticles exhibited desirable physicochemical properties, including uniform morphology, narrow particle size distribution, and enhanced stability[38]. Such similarities suggest that mangrove species, irrespective of geographical origin, possess a consistent capacity to facilitate the synthesis of stable and well-defined nanoparticles.

Overall, the consistency between the present findings and previous studies highlights the effectiveness of mangrove-derived phytochemicals in mediating nanoparticle synthesis and stabilisation. Variations in particle characteristics reported across studies may be attributed to differences in species, environmental conditions, and extraction protocols.

Characterization of Synthesized Silver Nanoparticles

The formation of silver nanoparticles (AgNPs) synthesized using the aqueous leaf extract of *Bruguiera gymnorrhiza* was confirmed through various characterization techniques. The results obtained from these analyses are discussed below.

UV–Visible Spectroscopy Analysis

UV-Vis (Ultraviolet-Visible) spectroscopy is one of the most widely used techniques for characterizing nanoparticles, especially metal nanoparticles such as silver (AgNPs). The appearance of a specific Surface Plasmon Resonance (SPR) peak in the UV-Vis spectrum confirms the formation of metallic nanoparticles. In our study, a peak was observed at 424

nm, confirming the synthesis of silver nanoparticles from *Bruguiera gymnorrhiza* (Fig. 3).

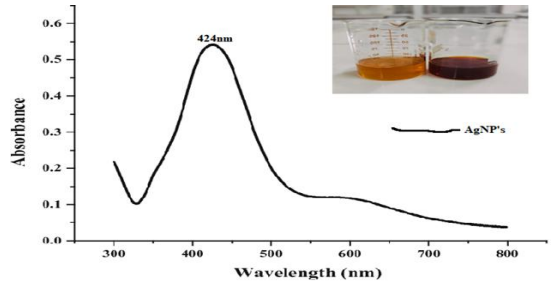

Figure 3. UV-visible spectra of the synthesized AgNPs from the aqueous leaf extract of *Bruguiera gymnorrhiza*

The UV–Visible spectroscopic results obtained in the present study are in good agreement with previous reports on mangrove-mediated synthesis of silver nanoparticles. For instance, AgNPs synthesized using *Rhizophora lamarckii* extracts have been reported to exhibit surface plasmon resonance (SPR) absorption maxima around 420 nm, corresponding to predominantly spherical nanoparticles[39]. The similarity in absorption peaks supports the findings of the current study and reinforces the role of mangrove-derived phytochemicals as efficient reducing and stabilizing agents in green nanoparticle synthesis.

Furthermore, studies on AgNPs synthesized from *Rhizophora stylosa* have demonstrated SPR bands in the range of 403–443 nm, which are strongly influenced by nanoparticle size, shape, and dispersion[40]. The observed SPR peak in the present study falls within this reported range, suggesting the formation of relatively uniform and spherical nanoparticles. Minor shifts in absorption maxima compared to earlier studies may be attributed to variations in particle size distribution, concentration of bioactive compounds, and experimental conditions.

Overall, the consistency of SPR characteristics across different mangrove species highlights the reliability of UV–Vis spectroscopy as a rapid and effective tool for confirming AgNP formation and provides further evidence for the reproducibility of mangrove-assisted green synthesis approaches.

Fourier Transform Infrared Spectroscopy (FTIR) Analysis

FTIR spectroscopy was performed to identify the functional groups present on the surface of the synthesized AgNPs from *Bruguiera gymnorrhiza*. The spectrum revealed characteristic peaks corresponding to C=O, C–H, and O–H groups like esters, ethers, or amides, confirming the formation of silver nanoparticles. The peak at 2361 cm^{-1} is attributed to CO_2, which is detected from the atmosphere. Prominent organic peaks observed at 1587 and 1284 cm^{-1} indicate the presence of biomolecules or stabilizing agents bound to the nanoparticle surface. Additionally, a low-frequency band at 449 cm^{-1} is characteristic of metallic silver, supporting the presence of Ag^0. These features collectively confirm that the nanoparticles are stabilized by organic compounds from the leaf extract. The FTIR analysis thus indicates the presence of hydroxyl, carbonyl, and amine groups, which likely functioned as reducing and capping agents during the synthesis of silver nanoparticles (Fig. 4).

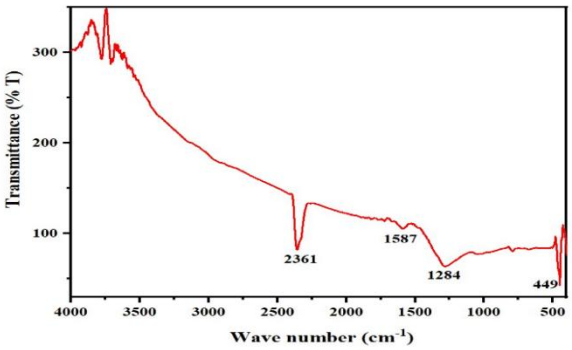

Figure 4. FTIR spectra of the synthesized AgNPs from the aqueous leaf extract of *Bruguiera gymnorhiza*

FTIR analysis provides valuable insight into the biomolecular interactions involved in nanoparticle synthesis and stabilization. Studies on AgNPs synthesized using *Sonneratia apetala* leaf extract have attributed characteristic absorption bands to functional groups such as amides and hydroxyl groups, indicating the involvement of proteins in nanoparticle capping and stabilization[9]. Similarly, FTIR spectra of AgNPs derived from *Rhynchosia capitata* have revealed bands corresponding to phenols, amines, and carbonyl compounds, highlighting the contribution of diverse phytoconstituents in nanoparticle formation[18].

In the present study involving *Bruguiera gymnorhiza*, the observed peaks corresponding to C=O, C–H, and O–H functional groups suggest the active participation of phytoconstituents such as proteins and polyphenols in the reduction of silver ions and stabilization of the nanoparticles. These biomolecules likely function as both reducing and capping agents, facilitating nanoparticle formation while preventing aggregation.

The combined evidence from functional group analysis and metal-specific vibrational signatures underscores the role of plant-derived biomolecules in governing the synthesis and stability of AgNPs.

Scanning-Electron-Microscopy (SEM) and Energy Dispersive X-ray (EDX) Analysis

SEM analysis revealed the morphology and size distribution of the synthesized silver nanoparticles of *Bruguiera gymnorrhiza*. The particles were predominantly spherical, with sizes ranging from approximately 10 to 50 nm. Both well-dispersed and aggregated nanoparticles were observed, indicating variability in particle distribution (Fig. 5).

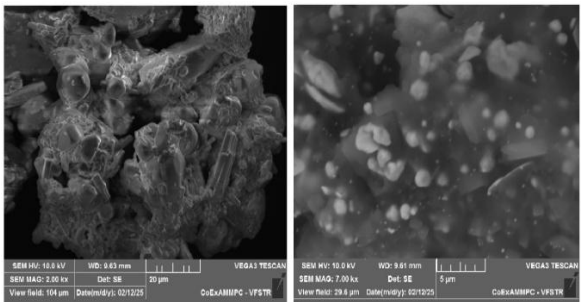

Figure 5. SEM images of synthesized AgNPs from the aqueous leaf extract of *Bruguiera gymnorrhiza.*

EDX analysis confirmed the elemental composition of the synthesized silver nanoparticles from *Bruguiera gymnorrhiza*, verifying successful formation and detecting any associated organic capping agents. A strong Ag peak observed at ~3 keV corresponds to metallic silver, while additional signals for C and O indicate the presence of organic molecules adsorbed on the nanoparticle surface (Fig. 6).

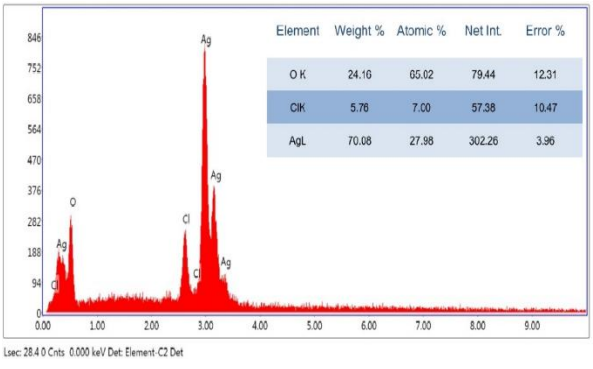

Figure 6. EDX analysis of synthesized AgNPs from the aqueous leaf extract of *Bruguiera gymnorrhiza,* showing its elemental composition.

SEM and EDX analyses together provide comprehensive insight into the morphology, distribution, and elemental composition of biosynthesized silver nanoparticles. SEM studies on AgNPs synthesized using *Rhynchosia capitata* and *Sonneratia apetala* have demonstrated predominantly spherical nanoparticles with relatively uniform distribution, indicating effective stabilization by plant-derived biomolecules[9,18]. In contrast, AgNPs from *Rhizophora apiculata* exhibited irregular shapes with particle sizes ranging from 35 to 100 nm, highlighting the influence of phytochemical composition on nanoparticle morphology[41].

In the present study involving *Bruguiera gymnorhiza*, SEM analysis revealed predominantly spherical nanoparticles with sizes ranging from 10 to 50 nm, suggesting controlled nucleation and growth mediated by bioactive compounds such as polyphenols and proteins. The relatively uniform dispersion of nanoparticles indicates reduced aggregation and enhanced stability, likely due to the capping action of these phytoconstituents.

EDX analysis further confirmed the elemental composition and purity of the synthesized nanoparticles. A strong characteristic signal around 3 keV, as reported for AgNPs from *Rhizophora apiculata*, corresponds to elemental silver[41]. In the present study, the prominent peak observed near 3 keV substantiates the successful formation of metallic silver nanoparticles. This characteristic signal is attributed to the optical absorption of metallic silver, typically observed around 3.0 keV due to surface plasmon-related interactions[42].

Overall, the combined SEM–EDX findings demonstrate that *B. gymnorhiza*-mediated synthesis yields well-defined, stable, and compositionally pure silver nanoparticles, emphasizing the effectiveness of plant-based green synthesis approaches.

Transmission Electron Microscopy (TEM) Analysis

TEM analysis of silver nanoparticles synthesized using *Bruguiera gymnorhiza* revealed well-dispersed particles with relatively uniform morphology. The nanoparticles were predominantly spherical in shape, with sizes ranging from 8 to 25 nm, with an average diameter of approximately 17 nm. The particles appeared discrete with minimal aggregation, indicating effective stabilization during synthesis.

The selected area electron diffraction (SAED) pattern (scale bar: 5 nm^{-1}) exhibited distinct concentric rings, confirming the crystalline nature of the nanoparticles. The sharp and continuous rings suggest the presence of

polycrystalline domains with well-defined lattice planes (Fig. 7).

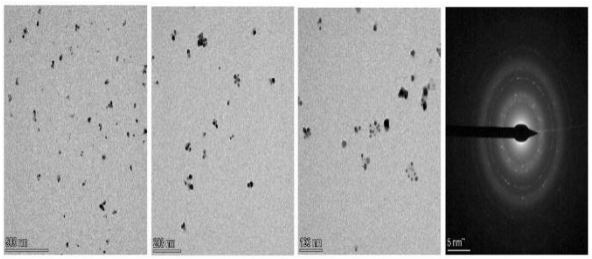

Figure 7. TEM images of synthesized AgNPs from the aqueous leaf extract of *Bruguiera gymnorrhiza.*

TEM analysis provides high-resolution evidence of nanoparticle size, morphology, and crystallinity. Earlier studies on mangrove-mediated synthesis have reported variation in particle sizes across species, including *Rhizophora mucronata* (60–95 nm), *Rhizophora apiculata* (19–42 nm), and *Rhizophora lamarckii* (12–28 nm) following the reduction of silver nitrate[43].

In comparison, the smaller size range (8–25 nm) observed in the present study suggests more efficient control over nucleation and growth processes. The predominantly spherical morphology and narrow size distribution indicate the role of phytoconstituents in directing nanoparticle formation and preventing aggregation. The crystalline nature confirmed by SAED further supports the structural integrity of the synthesized nanoparticles.

Variations in particle size and morphology among different studies may arise from differences in plant species, phytochemical composition, and synthesis conditions. The reduced particle size and improved dispersion observed in *B. gymnorhiza*-mediated synthesis highlight its potential for producing stable and uniformly distributed nanoparticles.

X-ray Diffraction (XRD) Analysis

The XRD pattern of the synthesized AgNPs from *Bruguiera gymnorrhiza* displayed distinct peaks at specific 2θ angles corresponding to the diffraction from crystallographic planes of silver's face-centered cubic (FCC) structure. The most intense peaks were observed at approximately 30°, 40°, and 50°, with additional smaller peaks distributed up to ~90°. The diffraction peaks were indexed to the (111), (200), and (220) planes, confirming the FCC crystalline nature of the silver nanoparticles (Fig. 8).

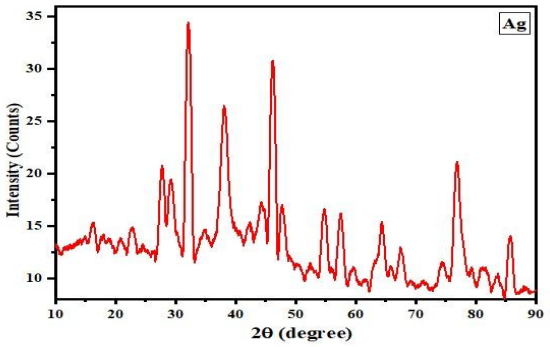

Figure 8. XRD spectra of the synthesized AgNPs from the aqueous leaf extract of *Bruguiera gymnorhiza*

X-ray diffraction (XRD) analysis provides critical information regarding the crystalline nature and phase structure of silver nanoparticles. Studies on AgNPs synthesized using *Rhizophora stylosa* leaf extract have reported well-defined diffraction peaks at 2θ values of 38.28°, 44.45°, 64.53°, and 77.53°, corresponding to the (111), (200), (220), and (311) planes of a face-centered cubic (fcc) structure of metallic silver[43]. In another study, AgNPs derived from *Rhizophora apiculata* exhibited multiple diffraction peaks at 2θ values including 23.52°, 27.79°, 32.19°, 33.29°, 37.62°, 38.08°, 38.57°, 44.13°, and 46.16°, indicating the crystalline nature of the synthesized nanoparticles[41].

In the present study involving *Bruguiera gymnorhiza*, the observed diffraction peaks corresponding to characteristic planes of silver confirm the formation of crystalline nanoparticles with an FCC structure. The presence of sharp and well-defined peaks indicates a high degree of crystallinity, while minor additional peaks, if present, may be attributed to residual organic compounds or bioactive molecules associated with the nanoparticle surface.

Variations in peak positions and intensities across different studies may result from differences in particle size, lattice strain, and the nature of capping agents derived from plant extracts. Overall, the XRD findings substantiate the crystalline structure and phase purity of the synthesized AgNPs, supporting their structural stability and potential applicability in biomedical fields.

Antibacterial Activity

Disc Diffusion Method

The antibacterial activity of antibiotics alone, AgNPs alone, and their combinations was evaluated against

Escherichia coli, Staphylococcus aureus, Pseudomonas aeruginosa, and *Bacillus subtilis*. The zone of inhibition values demonstrated that silver nanoparticles (AgNPs) enhanced the antibacterial efficacy of several antibiotics, exhibiting synergistic effects against both Gram-positive and Gram-negative bacteria (Table 2, Fig. 9). The most pronounced enhancement was observed with tetracycline, erythromycin, ciprofloxacin, and azithromycin, whereas vancomycin and nitrofurantoin showed comparatively limited inhibition.

Table 2. Zones of inhibition calculated in mm for antibacterial activity of silver nanoparticles synthesized from the aqueous leaf extract of *Bruguiera gymnorrhiza* in combination with various antibiotics.

Organisms	Antibiotics	Zone of Inhibition in mm		
		Only Antibiotic	AgNPs + Antibiotics	Only AgNPs
Escherichia coli	Tetracycline (30 mcg)	20	30	23
	Erythromycin (15 mcg)	35	35	12
	Ciprofloxacin (5 mcg)	28	30	15
	Azithromycin (15 mcg)	17	35	5
	Vancomycin (30 mcg)	28	27	15
	Nitrofurantoin (300 mcg)	38	38	8
Staphylococcus aureus	Tetracycline (30 mcg)	38	41	15
	Erythromycin (15 mcg)	35	40	15
	Ciprofloxacin (5 mcg)	31	33	15
	Azithromycin (15 mcg)	35	40	15
	Vancomycin (30 mcg)	27	34	12
	Nitrofurantoin (300 mcg)	38	42	12
Pseudomonas aeruginosa	Tetracycline (30 mcg)	24	30	18
	Erythromycin (15 mcg)	35	40	18
	Ciprofloxacin (5 mcg)	28	32	15
	Azithromycin (15 mcg)	32	36	15
	Vancomycin (30 mcg)	17	20	12
	Nitrofurantoin (300 mcg)	28	30	12
Bacillus subtilis	Tetracycline (30 mcg)	24	30	13
	Erythromycin (15 mcg)	35	40	13
	Ciprofloxacin (5 mcg)	35	40	15
	Azithromycin (15 mcg)	28	35	15
	Vancomycin (30 mcg)	17	20	12
	Nitrofurantoin (300 mcg)	28	32	12

The results of the present study highlight the significant antibacterial potential of *Bruguiera gymnorhiza*-mediated silver nanoparticles, which exhibited greater inhibitory activity than the crude plant extract against the tested bacterial strains. These results align with previous studies indicating that AgNPs are potent antibacterial agents capable of synergizing with conventional antibiotics. Specifically, Acharya et al. (2020)[44] reported that *B. gymnorrhiza* leaves can inhibit both Gram-positive bacteria, such as *S. aureus*, and Gram-negative bacteria, including *E. coli* and *P. aeruginosa*. Morones et al. (2005)[45] demonstrated that AgNPs interact with bacterial cell walls and membranes, causing structural damage and leakage of cellular contents. This mechanism likely underlies the enhanced activity observed in the present study, particularly against *E. coli* and *P. aeruginosa*, which are typically resistant due to their impermeable outer membranes. Overall, the *B. gymnorrhiza*-derived silver nanoparticles exhibited significant inhibitory activity against both Gram-positive and Gram-negative bacteria.

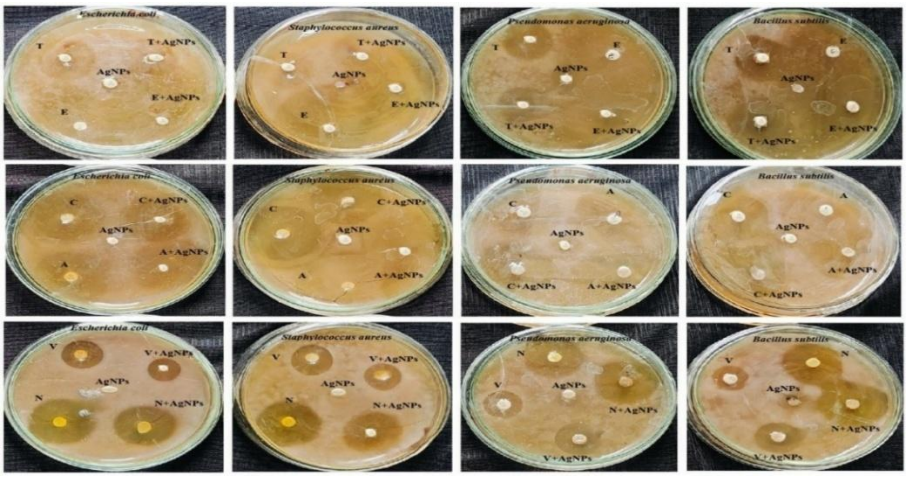

Figure 9. Antibacterial activity of silver nanoparticles synthesized from the aqueous leaf extract of *Bruguiera gymnorrhiza* in combination with various antibiotics, showing zones of inhibition on nutrient agar plates. T- tetracycline (30 mcg)**, E-** erythromycin (15 mcg)**, C-** ciprofloxacin (5 mcg)**, V-** vancomycin (30 mcg)**, N-** nitrofurantoin (300 mcg)**, and A-** azithromycin (15 mcg)**, AgNPs-** silver nanoparticles**.**

Antioxidant activity

DPPH Radical Scavenging Assay

The antioxidant activity of *Bruguiera gymnorrhiza*-derived silver nanoparticles (AgNPs) was evaluated using the DPPH radical scavenging assay and compared with the standard ascorbic acid. The results demonstrated a concentration-dependent increase in percentage inhibition for both AgNPs and ascorbic acid. At lower concentrations, AgNPs exhibited moderate radical scavenging activity, with inhibition values significantly lower than those of the standard. However, with increasing concentration, the scavenging activity of AgNPs improved steadily, reaching appreciable levels at higher concentrations. Ascorbic acid consistently exhibited higher inhibition across all tested concentrations. These findings indicate that while AgNPs possess notable antioxidant activity, their efficacy is comparatively lower than that of the standard antioxidant (Table 3, Fig.10).

The observed antioxidant activity of *B. gymnorrhiza*-derived AgNPs can be attributed to the presence of phytochemicals from the plant extract that act as reducing and capping agents during nanoparticle synthesis. Biomolecules such as flavonoids, phenolics, and tannins are known to donate electrons or hydrogen atoms to neutralize free radicals, thereby contributing to the radical scavenging effect[46,47]. The concentration-dependent increase in inhibition is consistent with previous reports on plant-mediated AgNPs, where higher nanoparticle concentrations provide more active sites for interaction with free radicals[48]. Similar observations have been reported for mangrove-derived AgNPs, which exhibit moderate antioxidant activity. However, the relatively lower activity compared to ascorbic acid is expected, as ascorbic acid is a well-established potent antioxidant, whereas AgNPs rely on surface-bound phytochemicals for their radical scavenging activity[49].

Table 3. Percentage inhibition of DPPH radical scavenging activity of silver nanoparticles synthesized from the aqueous leaf extract of *Bruguiera gymnorrhiza*.

Conc. (µg/mL)	% DPPH Radical Scavenging Activity of AgNPs from *Bruguiera gymnorrhiza*	IC_{50} of AgNPs	% DPPH Radical Scavenging Activity of Ascorbic Acid Standard	IC_{50} of Ascorbic acid
10	42.62±0.30	22.38± 0.30	37.66± 0.06	17.88± 0.20
20	51.04±0.52		55.59± 0.21	
50	63.44±0.10		74.39± 0.21	
75	70.13±0.25		87.19± 0.32	
100	77.31±0.21		92.49± 0.06	
*Each value is represented as mean ± SD (n=3).				

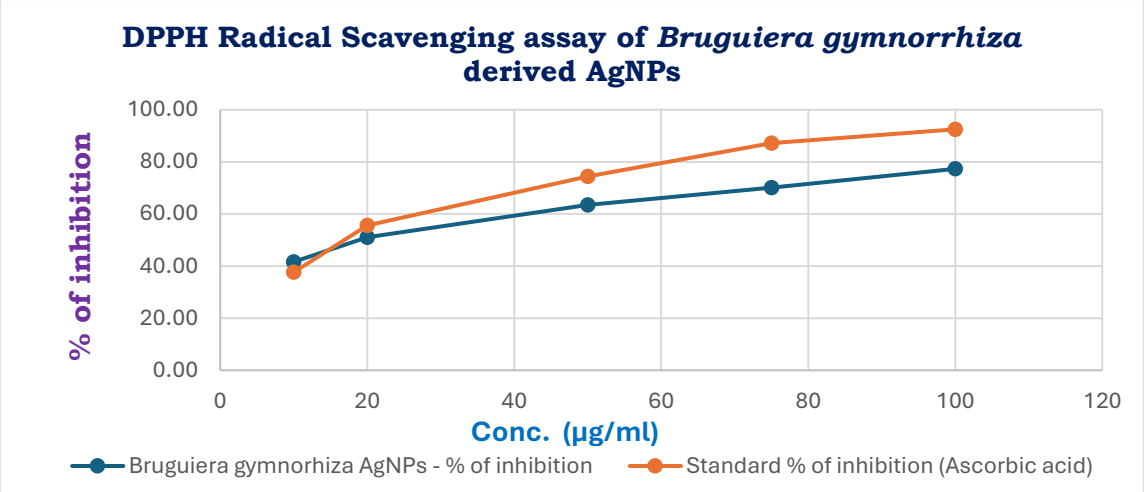

Figure 10. DPPH Assay of *Bruguiera gymnorrhiza*–Derived Silver Nanoparticles

FRAP Assay

The Ferric Reducing Antioxidant Power (FRAP) assay was performed to evaluate the antioxidant potential of *Bruguiera gymnorrhiza*-derived silver nanoparticles (AgNPs) compared with the standard antioxidant ascorbic acid. Both AgNPs and ascorbic acid exhibited a concentration-dependent increase in reducing power. At lower concentrations, AgNPs exhibited moderate FRAP values, significantly lower than those of ascorbic acid. However, with increasing concentration, the reducing power of AgNPs increased steadily, reaching values comparable at the highest tested concentration. Ascorbic acid consistently demonstrated higher reducing activity across all concentrations, indicating that although AgNPs possess notable reducing ability, their antioxidant potential is comparatively lower than that of the standard (Table 4, Fig. 11).

The observed reducing power of *B. gymnorrhiza*-derived AgNPs can be attributed to the presence of phytochemicals from the plant extract that act as reducing and capping agents during nanoparticle synthesis. Biomolecules such as polyphenols, flavonoids, and tannins are known to donate electrons, facilitating the reduction of ferric (Fe^{3+}) to ferrous (Fe^{2+}) ions and thereby contributing to antioxidant activity[47]. The concentration-dependent increase in FRAP values is consistent with previous reports on plant-mediated AgNPs, where higher nanoparticle concentrations provide more active sites for electron transfer[48]. Although the activity of AgNPs was lower than that of ascorbic acid, their moderate reducing potential highlights their significance as multifunctional agents with both antimicrobial and antioxidant properties. Similar observations have been reported for mangrove-derived AgNPs, where moderate FRAP activity was noted, suggesting that the antioxidant potential is largely influenced by the phytochemical composition of the plant extract used in synthesis[49].

Table 4. Ferric reducing antioxidant power (FRAP) activity, expressed as percentage inhibition, of silver nanoparticles synthesized from the aqueous leaf extract of *Bruguiera gymnorrhiza*.

Conc. (µg/mL)	FRAP Activity of AgNPs from *Bruguiera gymnorrhiza* (µg/mL)	IC_{50} of AgNPs	FRAP Activity of Ascorbic acid standard (µg/mL)	IC_{50} of Ascorbic acid
10	13.98±1.05	66.92± 0.67	7.171±0.29	46.59± 0.49
20	23.59±0.43		18.35±0.46	
50	42.81±0.70		44.62±0.64	
75	50.38±0.44		71.55±0.79	
100	71.55±0.57		96.15±0.67	
*Each value is represented as mean ± SD (n = 3).				

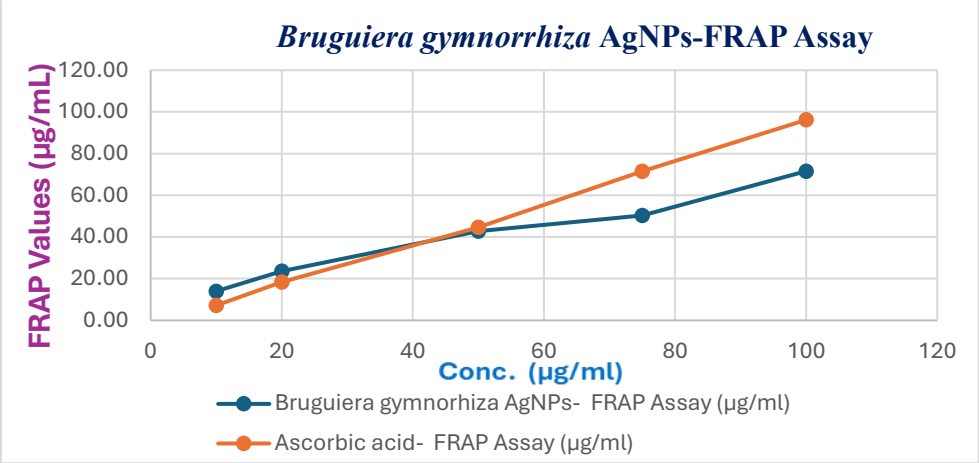

Figure 11. FRAP Assay for *Bruguiera gymnorrhiza*–Derived Silver Nanoparticles

Nitric Oxide (NO) Scavenging Assay

The Nitric Oxide (NO) scavenging activity of *Bruguiera gymnorrhiza*-derived silver nanoparticles (AgNPs) was evaluated and compared with the standard antioxidant, ascorbic acid. Both AgNPs and ascorbic acid exhibited a concentration-dependent increase in NO scavenging activity. At lower concentrations, AgNPs showed moderate inhibition values that were consistently lower than those of ascorbic acid. However, with increasing concentration, the scavenging activity of AgNPs improved significantly, reaching higher percentage inhibition at the maximum tested concentration. Ascorbic acid consistently demonstrated superior activity across all concentrations, indicating that although AgNPs possess notable NO scavenging potential, their efficacy is comparatively lower than that of the standard antioxidant (Table 5, Fig. 12).

The observed NO scavenging activity of *B. gymnorrhiza*-derived AgNPs is in agreement with previous reports on plant-mediated nanoparticle synthesis. Oke et al. (2021)[50] demonstrated that AgNPs exhibit significant NO scavenging activity, attributed to their high phenolic and flavonoid content. These plant-derived nanoparticles are capped and stabilized by biomolecules such as phenolics, flavonoids, and tannins, which can donate electrons or hydrogen atoms to neutralize free radicals. Similarly, Antony et al. (2024)[51] reported that AgNPs synthesized from *Rhizophora apiculata* extracts showed moderate antioxidant activity, highlighting the role of mangrove phytochemicals in enhancing bioactivity. Furthermore, Elangovan et al. (2024)[52] observed strong free radical-scavenging activity, including NO inhibition, emphasizing the potential of plant-based systems as effective sources of functional nanoparticles.

Table 5. The % inhibition of nitric oxide (NO) assay from *Bruguiera gymnorrhiza*–derived silver nanoparticles

Conc. (µg/mL)	% NO Scavenging Activity of AgNPs from *Bruguiera gymnorrhiza*	IC_{50} of AgNPs	% NO Scavenging Activity of Ascorbic acid standard	IC_{50} of Ascorbic acid
10	31.84±0.40	36.50± 0.99	38.69±0.40	16.42± 0.45
20	45.11±1.05		56.31±0.55	
50	59.82±0.30		74.67±0.15	
75	68.68±0.43		86.38±0.30	
100	81.94±0.15		92.77±0.55	
*Each value is represented as mean ± SD (n=3).				

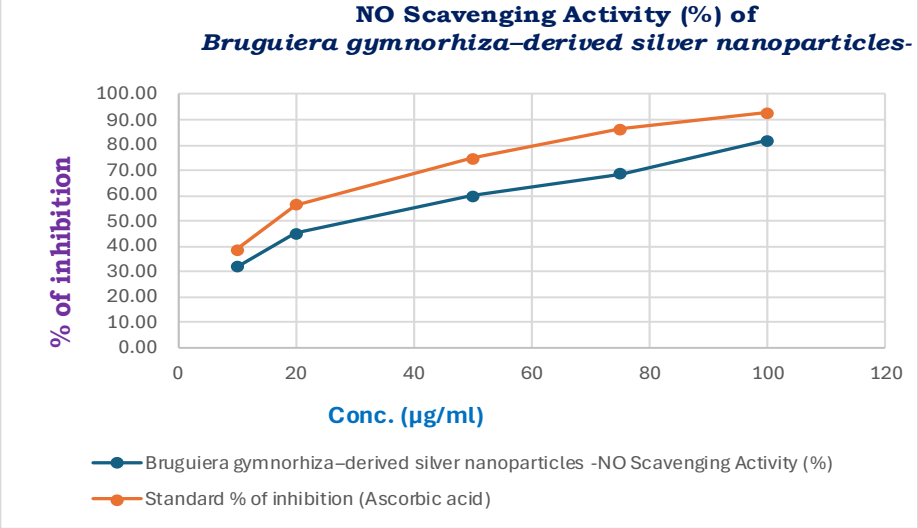

Figure 12. Nitric Oxide (NO) Scavenging Assay for *Bruguiera gymnorrhiza*–Derived Silver Nanoparticles

Antidiabetic activity

Assay of α-Amylase Inhibition Activity

The α-amylase inhibitory activity of *Bruguiera gymnorrhiza*-derived silver nanoparticles (AgNPs) was evaluated and compared with the standard antidiabetic drug, acarbose. Both AgNPs and acarbose exhibited a concentration-dependent increase in inhibition. At lower concentrations (2–4 µg/mL), AgNPs showed moderate inhibitory activity, whereas acarbose demonstrated comparatively higher inhibition. With increasing concentration up to 15 µg/mL, the inhibitory activity of AgNPs increased steadily, reaching a higher percentage inhibition at the maximum tested concentration; however, acarbose consistently exhibited superior inhibition across all concentrations. Overall, AgNPs displayed significant α-amylase inhibitory activity, although lower than that of the standard drug (Table 6, Fig. 13).

The observed α-amylase inhibition sugests the potential antidiabetic properties of *B. gymnorrhiza*-derived AgNPs, as inhibition of α-amylase delays carbohydrate digestion and glucose absorption, thereby reducing postprandial hyperglycemia[53]. This activity can be attributed to the phytochemicals present in the plant extract, which act as reducing and capping agents during nanoparticle synthesis. Biomolecules such as flavonoids, tannins, and phenolic compounds are known to interact with digestive enzymes and inhibit their activity[54]. Similar findings were reported by Antony et al. (2024)[51], where AgNPs synthesized from *Rhizophora apiculata* extracts exhibited moderate α-amylase inhibitory activity, supporting the present results.

Table 6. Percentage inhibition of α-amylase activity by silver nanoparticles synthesized from the aqueous leaf extract of *Bruguiera gymnorrhiza*.

Conc. (µg/mL)	% inhibition of α-amylase activity by AgNPs from *Bruguiera gymnorrhiza*	IC_{50} of AgNPs	% inhibition of α-amylase activity by Standard Acarbose	IC_{50} of Acarbose standard
2	18.34±0.35	11.29± 0.10	20.68±0.24	7.77± 0.02
4	25.53±0.13		39.48±0.47	
8	39.95±0.93		50.67±0.55	
10	47.75±1.45		62.44±0.07	
15	60.75±0.52		77.39±0.20	
*Each value is represented as mean ± SD (n=3).				

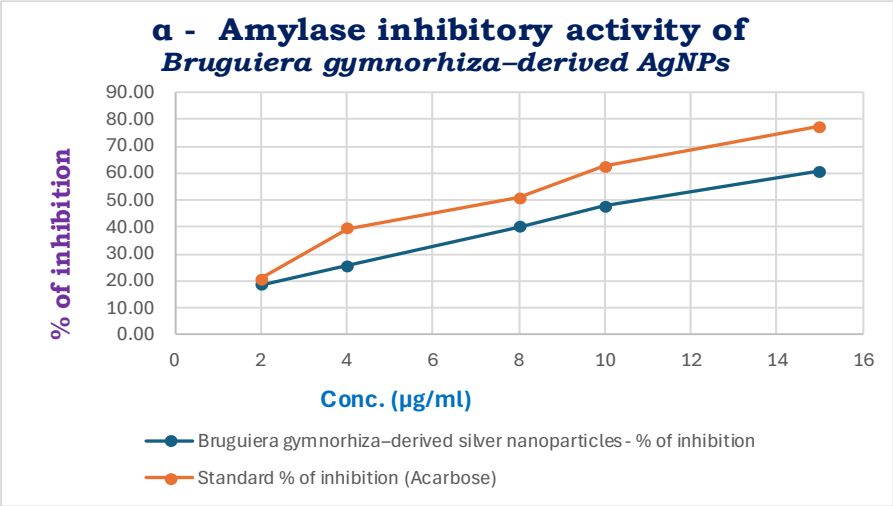

Figure 13. α-Amylase inhibitory activity of silver nanoparticles synthesized from the aqueous leaf extract of *Bruguiera gymnorrhiza*.

Assay of α-Glucosidase Inhibition Activity

The α-glucosidase inhibitory activity of *Bruguiera gymnorrhiza*-derived silver nanoparticles (AgNPs) was evaluated and compared with the standard antidiabetic drug, acarbose. Both AgNPs and acarbose exhibited a concentration-dependent increase in inhibition. At lower concentrations (2–4 µg/mL), AgNPs showed moderate inhibitory activity, whereas acarbose demonstrated comparatively higher inhibition. With increasing concentration up to 15 µg/mL, the inhibitory activity of AgNPs increased progressively, reaching higher percentage inhibition at the maximum tested concentration; however, acarbose consistently exhibited superior inhibition across all concentrations. Overall, AgNPs demonstrated significant α-glucosidase inhibitory activity, although lower than that of the standard (Table 7, Fig. 14).

The observed α-glucosidase inhibition indicates the potential antidiabetic properties of *B. gymnorrhiza*-derived AgNPs. α-Glucosidase is a key enzyme involved in carbohydrate metabolism, responsible for the breakdown of disaccharides into glucose; its inhibition delays glucose absorption and reduces postprandial hyperglycemia[53]. This inhibitory activity can be attributed to the phytochemical constituents present in the plant extract, which act as reducing and capping agents during nanoparticle synthesis. Biomolecules such as phenolic compounds, flavonoids, and terpenoids are known to interact with digestive enzymes and inhibit their activity. González-Garibay et al. (2025)[55] reported that biosynthesized AgNPs exhibit α-glucosidase inhibition due to phytochemical coatings that enhance enzyme interaction. Similarly, Vishwakarma et al. (2025)[56] demonstrated strong α-glucosidase and α-amylase inhibition by plant-mediated AgNPs, highlighting the role of bioactive compounds in enhancing antidiabetic efficacy. Jini et al. (2022)[57] also reported significant inhibition of starch digestion and α-glucosidase activity by garlic-derived AgNPs, attributing the effect to the presence of phenols and terpenoids.

Table 7: Percentage inhibition of α-glucosidase activity by silver nanoparticles synthesized from the aqueous leaf extract of *Bruguiera gymnorhiza*.

Conc. (µg/mL)	% inhibition of α-glucosidase activity by AgNPs from *Bruguiera gymnorrhiza*	IC_{50} of AgNPs	% inhibition of α-glucosidase activity by Acarbose standard	IC_{50} of Acarbose standard
2	15.39±0.38	12.02±0.06	21.84±0.45	7.77± 0.06
4	23.92±0.38		34.27±0.53	
8	37.32±0.32		52.16±0.38	
10	48.13±0.32		66.16±0.46	
15	56.62±0.34		76.29±0.19	
*Each value is represented as mean ± SD (n=3).				

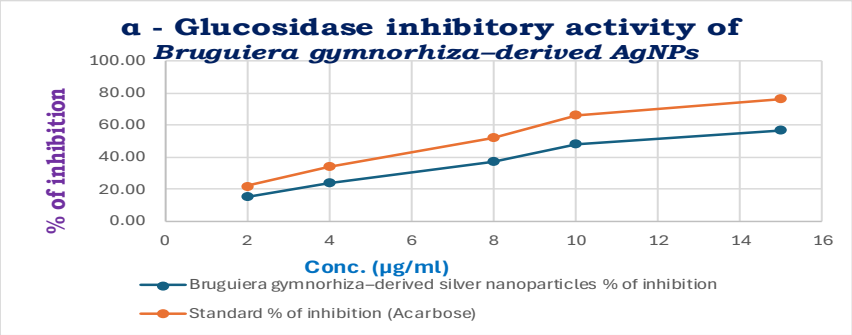

Figure 14. α-Glucosidase inhibitory activity of silver nanoparticles synthesized from the aqueous leaf extract of *Bruguiera gymnorrhiza*.

Glucose Uptake by Yeast Cells Method

The yeast glucose uptake assay was performed at glucose concentrations of 5 mM, 10 mM, and 20 mM to evaluate the effect of *Bruguiera gymnorrhiza*-derived silver nanoparticles (AgNPs) in comparison with the standard drug, metronidazole, across concentrations ranging from 10 to 50 µg/mL. Both AgNPs and the standard promoted glucose uptake in yeast cells; however, metronidazole consistently exhibited higher uptake values under all tested conditions. AgNPs demonstrated moderate glucose uptake activity, with values increasing progressively with concentration and reaching higher uptake at the maximum tested levels. Despite this improvement, the activity remained lower than that of the standard. Overall, the results indicate that AgNPs are capable of enhancing glucose uptake in yeast cells, albeit less effectively than metronidazole. On the other hand, an inverse relationship to the molar concentration of glucose was observed when glucose uptake by yeast cells was compared among 5 mM, 10 mM, and 20 mM for the same amount of AgNPs concentration. The results indicate that the lower the concentration of glucose in the solution, the higher the uptake by yeast cells. (Tables 8, 9, and 10; Fig. 15, 16 and 17).

Table 8. Glucose uptake by yeast cells at 5 mM glucose concentration following treatment with silver nanoparticles synthesized from the aqueous leaf extract of *Bruguiera gymnorrhiza*.

Conc. (µg/ml)	Standard (Metronidazole)	*Bruguiera gymnorrhiza*–derived silver nanoparticles
10	18.44±0.42	12.24±0.41
20	31.02±0.41	21.29±0.42
30	43.54±0.42	33.06±0.41
40	55.37±0.62	41.90±0.31
50	64.01±0.31	53.47±0.41

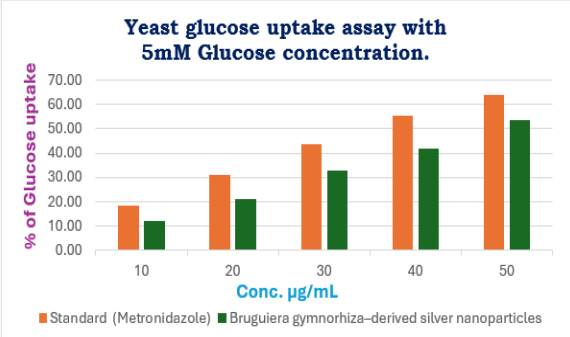

Figure 15. Glucose Uptake by Yeast Cells Assay with 5 mM Glucose Concentration

Table 9. Glucose uptake by yeast cells at 10 mM glucose concentration following treatment with silver nanoparticles synthesized from the aqueous leaf extract of *Bruguiera gymnorrhiza*.

Conc. (µg/ml)	Standard (Metronidazole)	*Bruguiera gymnorrhiza*–derived silver nanoparticles
10	12.64±.23	10.37±0.39
20	19.11±.39	17.98±0.37
30	24.00±0.39	25.48±0.39
40	30.22±0.44	31.80±0.37
50	41.19±.26	36.49±0.56

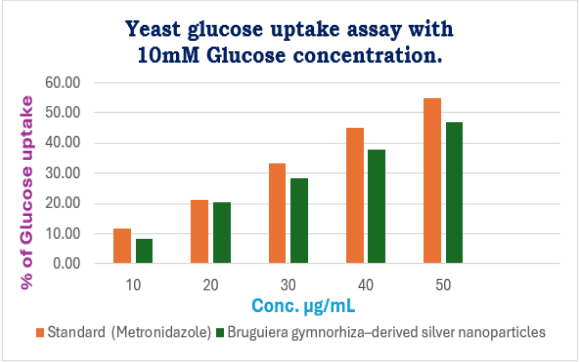

Figure 16. Glucose Uptake by Yeast Cells Assay with 10 mM Glucose Concentration

Table 10. Glucose uptake by yeast cells at 20 mM glucose concentration following treatment with silver nanoparticles synthesized from the aqueous leaf extract of *Bruguiera gymnorrhiza*.

Conc. (µg/ml)	Standard (Metronidazole)	*Bruguiera gymnorrhiza*–derived silver nanoparticles
10	8.99±0.29	5.37±0.29
20	16.85±0.23	15.31±0.28
30	25.84±0.17	23.54±0.23
40	34.36±0.23	32.20±0.17
50	43.90±0.28	39.62±0.33

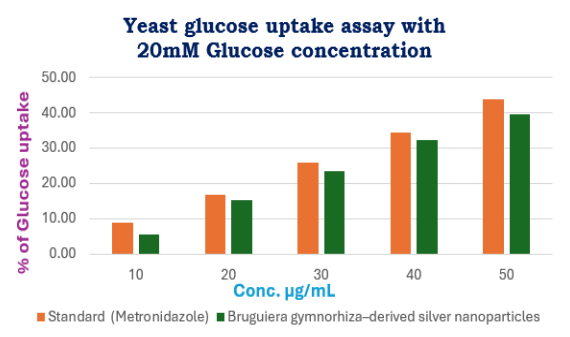

Figure 17. Glucose Uptake by Yeast Cells Method with 20 mM Glucose Concentration

The moderate activity observed for *B. gymnorrhiza*-derived AgNPs can be attributed to the phytochemicals present in the mangrove extract used during nanoparticle synthesis. Biomolecules such as flavonoids and phenolic compounds are known to enhance glucose uptake by modulating glucose transporter activity and reducing oxidative stress[58]. These compounds, acting as capping agents on the nanoparticle surface, may interact with yeast cell membranes and improve glucose transport efficiency. González-Garibay et al. (2025)[55] reported that plant-mediated AgNPs can enhance glucose uptake in both yeast and mammalian systems, supporting their potential antidiabetic applications. As per Bhav et al. (2024)[59], the relatively lower IC_{50} value observed for AgNPs compared to the plant extract suggests enhanced potency following nanoparticle synthesis. This improved activity can be attributed to the unique physicochemical properties of nanoparticles, particularly their high surface-to-volume ratio, which facilitates greater interaction with cellular components involved in glucose transport and metabolism[60,61]. The findings from the glucose uptake assay highlight the antidiabetic potential of *B. gymnorrhiza*-derived AgNPs, suggesting their ability to promote glucose utilization through mechanisms analogous to insulin-like activity[62]. Although less potent than the standard drug, their phytochemical-mediated activity underscores their potential for nutraceutical and pharmaceutical applications.

CONCLUSION

The green synthesis of silver nanoparticles using the aqueous leaf extract of *Bruguiera gymnorrhiza* represents an eco-friendly and sustainable alternative to conventional physicochemical methods. This approach is advantageous due to its cost-effectiveness, reduced environmental impact, and operational simplicity, making it a promising strategy for nanoparticle production. The presence of diverse phytochemicals, including polyphenols, alkaloids, flavonoids, and reducing sugars, facilitates the reduction of silver ions (Ag^+) to stable silver nanoparticles (AgNPs). The successful synthesis and physicochemical properties of the AgNPs were confirmed through multiple characterization techniques. UV–Visible spectroscopy revealed a characteristic surface plasmon resonance (SPR) peak at 424 nm, confirming nanoparticle formation, while FTIR analysis identified functional groups involved in reduction and stabilization. X-ray diffraction (XRD) confirmed the crystalline nature of the nanoparticles, Scanning Electron Microscopy (SEM) provided insights into their morphology, size, and shape. Furthermore, energy dispersive X-ray (EDX) analysis verified the elemental composition, confirming the presence of silver, and TEM confirmed the average nanoparticle size and shape. Collectively, these characterization results validate the successful synthesis of AgNPs.

The synthesized nanoparticles exhibited enhanced biological activities, including antibacterial, antioxidant, and antidiabetic effects, demonstrating significantly higher activity compared to the plant extract alone. This enhanced bioactivity can be attributed to the synergistic interaction between silver and surface-bound phytochemicals. The green synthesis approach also offers significant potential for large-scale production, addressing the increasing demand for sustainable nanotechnology applications while minimizing the use of toxic chemicals and energy-intensive processes. Future studies should focus on exploring the therapeutic potential of *B. gymnorrhiza*-derived AgNPs and elucidating their mechanistic pathways through in vivo models, which will further support their application in biomedical and pharmaceutical fields.

REFERENCES

1. Ritu, Verma KK, Das A, Chandra P. Phytochemical-based synthesis of silver nanoparticle: mechanism and potential applications. BioNanoScience. 2023; 13(3):1359-80. https://doi.org/10.1007/s12668-023-01125-x
2. Singh J, Kumar A, Singh A, Nayal AS, Pratap D. Green synthesized silver and zinc oxide nanoparticles with antifungal, DNA protection, DNA cleavage, and cytotoxic activities. Scientific Reports. 2026; 16: 10573. https://doi.org/10.1038/s41598-026-45745-1
3. da Silva MD, Muraro PC, de Oliveira JS, Vizzotto B, Baldez RN, da Silva WL. Silver Nanoparticles: Synthesis, Characterization, and Biological Applications. In Applications of Nanotechnology in Plant Disease Management 2026 (pp. 337-360). Singapore: Springer Nature Singapore. https://doi.org/10.1007/978-981-95-4913-9_13
4. Jiang X, Khan S, Dykes A, Stulz E, Zhang X. Biogenic synthesis of silver nanoparticles and their diverse biomedical applications. Molecules. 2025; 30(15):3104. https://doi.org/10.3390/molecules30153104
5. Liaqat N, Jahan N, Anwar T, Qureshi H. Green synthesized silver nanoparticles: Optimization, characterization, antimicrobial activity, and cytotoxicity study by hemolysis assay. Frontiers in chemistry. 2022; 10:952006. https://doi.org/10.3389/fchem.2022.952006
6. Sivaperumal P, Kamala K, Ganapathy DM, Dharani G, Sundarrajan S, Ramakrishna S. Fabrication of AgNPs mediated fibrous membrane from Rhizophora mucronata mangrove plant extract for biological properties. Journal of Drug Delivery Science and Technology. 2023; 86:104710. https://doi.org/10.1016/j.jddst.2023.104710
7. Dubey RK, Shukla S, Hussain Z. Green synthesis of silver nanoparticles: A sustainable approach with diverse applications. Zhongguo Ying Yong Sheng Li Xue Za Zhi. 2023; 39: e20230007.
8. Fahim M, Shahzaib A, Nishat N, Jahan A, Bhat TA, Inam A. Green synthesis of silver nanoparticles: A comprehensive review of methods, influencing factors, and applications. JCIS Open. 2024; 16: 100125. https://doi.org/10.1016/j.jciso.2024.100125
9. Nagababu P, Rao VU. Pharmacological assessment, green synthesis and characterization of silver nanoparticles of Sonneratia apetala Buch. -Ham. leaves. Journal of Applied Pharmaceutical Science. 2017; 7(8):175-82. https://dx.doi.org/10.7324/JAPS.2017.70824
10. Willian N, Pardi H, Fitriyah D, Yetti RD. Silver Nanoparticles In Cosmetics: A New Challenge Using Marine Resources. InBIO Web of Conferences 2023 (Vol. 79, p. 12004). EDP Sciences. https://doi.org/10.1051/bioconf/20237912004
11. Bayık GD, Baykal B. Optimization of green synthesis parameters of silver nanoparticles with factorial design for dye removal. Gazi University Journal of Science Part A: Engineering and Innovation. 2023;10(3):327-40. https://doi.org/10.54287/gujsa.1294774
12. Fares A, Mahdy A, Ahmed G. Unraveling the mysteries of silver nanoparticles: synthesis, characterization, antimicrobial effects and uptake translocation in plant—a review. Planta. 2024; 260(1):7. https://doi.org/10.1007/s00425-024-04439-6
13. Selvaraj A, Murthy KM, Rajmohan R. Omnipotent plant sources assisted green synthesis of Silver Nanoparticle-A promising Chemical Sensing tool. Journal of the Turkish Chemical Society Section A: Chemistry. 2024; 11(2):899-918. https://doi.org/10.18596/jotcsa.1370240
14. Asiya SI, Sarangapani A. A review of the antimicrobial benefits of naturally extracted nanomaterials. Int J Adv Appl Sci. 2024; 13(2): 2. 10.11591/ijaas.v13.i2.pp313-324
15. Ananda MB, Sanjaya FA, Widiyanti P. Fast microwave-assisted green synthesis of silver nanoparticles using low concentration of seminyak (Champeria sp.) leaf extract. Indonesian Journal of Chemistry. 2023;23(2). http://repository.unair.ac.id/id/eprint/126742
16. Nikunj Moudgil and Roopali Sharma. Green synthesis of silver nanoparticles: Characterization and therapeutic applications. Int. J. Biosci. Biochem. 2024; 6(2):23-33. 10.33545/26646536.2024.v6.i2a.79

17. Eker F, Akdaşçi E, Duman H, Bechelany M, Karav S. Green synthesis of silver nanoparticles using plant extracts: A comprehensive review of physicochemical properties and multifunctional applications. International Journal of Molecular Sciences. 2025; 26(13):6222. https://doi.org/10.3390/ijms26136222
18. Ullah Z, Iqbal J, Gul F, Abbasi BA, Kanwal S, Elsadek MF, Ali MA, Iqbal R, Elsalahy HH, Mahmood T. Biogenic synthesis, characterization, and in vitro biological investigation of silver oxide nanoparticles (AgONPs) using Rhynchosia capitata. Scientific Reports. 2024; 14(1):10484. https://doi.org/10.1038/s41598-024-60694-3
19. Singh H, Desimone MF, Pandya S, Jasani S, George N, Adnan M, Aldarhami A, Bazaid AS, Alderhami SA. Revisiting the green synthesis of nanoparticles: uncovering influences of plant extracts as reducing agents for enhanced synthesis efficiency and its biomedical applications. International journal of nanomedicine. 2023; 4727-4750. https://doi.org/10.2147/IJN.S419369
20. Rizwana H, Aljowaie RM, Al Otibi F, Alwahibi MS, Alharbi SA, Al Asmari SA, Aldosari NS, Aldehaish HA. Antimicrobial and antioxidant potential of the silver nanoparticles synthesized using aqueous extracts of coconut meat (Cocos nucifera L). Scientific reports. 2023; 13(1):16270. https://doi.org/10.1038/s41598-023-43384-4
21. Guzmán MG, Dille J, Godet S. Synthesis of silver nanoparticles by chemical reduction method and their antibacterial activity. Int J Chem Biomol Eng. 2009 Jan 1;2(3):104-11.
22. Gulcin İ, Alwasel SH. DPPH radical scavenging assay. Processes. 2023;11(8):2248. https://doi.org/10.3390/pr11082248
23. Ahmed AM. History of diabetes mellitus. Saudi Medical Journal. 2002; 23(4):373-8.
24. Shaikh JR, Patil M. Qualitative tests for preliminary phytochemical screening: An overview. International journal of chemical studies. 2020; 8(2):603-8. https://doi.org/10.22271/chemi.2020.v8.i2i.8834
25. Riyadi PH, Tanod WA, Dewanto DK, Herawati VE, Susanto E, Aisiah S. Chemical profiles and antioxidant properties of Bruguiera gymnorrhiza fruit extracts from Central Sulawesi, Indonesia. Food Research. 2021;5(3):37-47. https://doi.org/10.26656/fr.2017.5(S3).007
26. Yamauchi M, Kitamura Y, Nagano H, Kawatsu J, Gotoh H. DPPH measurements and structure—Activity relationship studies on the antioxidant capacity of phenols. Antioxidants. 2024; 13(3):309. https://doi.org/10.3390/antiox13030309
27. Benzie IF, Strain JJ. The ferric reducing ability of plasma (FRAP) as a measure of "antioxidant power": the FRAP assay. Analytical biochemistry. 1996; 239(1):70-6. https://doi.org/10.1006/abio.1996.0292
28. Banerjee A, Dasgupta N, De B. In vitro study of antioxidant activity of Syzygium cumini fruit. Food chemistry. 2005; 90(4):727-33. https://doi.org/10.1016/j.foodchem.2004.04.033
29. Bryan NS, Grisham MB. Methods to detect nitric oxide and its metabolites in biological samples. Free radical biology and medicine. 2007; 43(5):645-57. https://doi.org/10.1016/j.freeradbiomed.2007.04.026
30. Ali H, Houghton PJ, Soumyanath A. α-Amylase inhibitory activity of some Malaysian plants used to treat diabetes; with particular reference to Phyllanthus amarus. Journal of Ethnopharmacology. 2006; 107(3):449-55. https://doi.org/10.1016/j.jep.2006.04.004
31. Kim JS, Hyun TK, Kim MJ. The inhibitory effects of ethanol extracts from sorghum, foxtail millet and proso millet on α-glucosidase and α-amylase activities. Food Chemistry. 2011; 124(4):1647-51. https://doi.org/10.1016/j.foodchem.2010.08.020
32. Daksha Gupta, Chandrashekher KS, Pal G. In vitro antidiabetic activity of pentacyclic triterpenoids and fatty acid esters from Bauhinia purpurea. International Journal of Pharmacology and Pharmaceutical Technology. 2013;2(1):25-8.
33. Rahman MA, Ahmed A, Shahid IZ. Phytochemical and pharmacological properties of Bruguiera gymnorrhiza root extract. International Journal of Pharmaceutical Research. 2011; 3(3) 63-67

34. Karim MA, Islam MA, Islam MM, Rahman MS, Sultana S, Biswas S, et al. Evaluation of antioxidant, anti-hemolytic, cytotoxic effects and anti-bacterial activity of selected mangrove plants (Bruguiera gymnorrhiza and Heritiera littoralis) in Bangladesh. Clinical Phytoscience. 2020;6. Available from: https://doi.org/10.1186/s40816-020-0152-9.
35. Khadeeja S, Ragunathan R, Johney J, Muthusamy K. Phytochemical analysis, antimicrobial and antioxidant activity of mangrove plants Bruguiera gymnorrhiza (L.) Lam. and Excoecaria agallocha L. Indian Journal of Science and Technology. 2022 Dec 15;15(47):2594-604. https://doi.org/10.17485/IJST/v15i47.1633
36. Bibi Sadeer N, Sinan KI, Cziáky Z, Jekő J, Zengin G, Jeewon R, Abdallah HH, Rengasamy KR, Fawzi Mahomoodally M. Assessment of the pharmacological properties and phytochemical profile of Bruguiera gymnorhiza (L.) lam using in vitro studies, in silico docking, and multivariate analysis. Biomolecules. 2020;10(5):731. https://doi.org/10.3390/biom10050731.
37. Bhuvaneswari R, Xavier RJ, Arumugam M. Biofabrication and its in vitro toxicity mechanism of silver nanoparticles using Bruguiera cylindrica leaf extract. Karbala International Journal of Modern Science. 2015;1(2):129-34. https://doi.org/10.1016/j.kijoms.2015.08.003
38. Willian N, Syukri Z, Labanni A, Arief S. Bio-Friendly synthesis of silver nanoparticles using mangrove Rhizophora stylosa leaf aqueous extract and its antibacterial and antioxidant activity. Rasayan Journal of Chemistry. 2020;13(3):1478-85. https://doi.org/10.12688/f1000research.54661.2
39. Rahman A, Kumar S, Bafana A, et al.: Biosynthetic conversion of Ag^{+} to highly stable Ag^{0} nanoparticles by wild-type and cell wall-deficient strains of Chlamydomonas reinhardtii. *Molecules.* 2019; 24. https://doi.org/10.3390/molecules24010098
40. Mittal AK, Chisti Y, Banerjee UC: Synthesis of metallic nanoparticles using plant extracts. *Biotechnol. Adv.* 2013; 31:346–356. https://doi.org/10.1016/j.biotechadv.2013.01.003
41. Alsareii SA, Manaa Alamri A, AlAsmari MY, Bawahab MA, Mahnashi MH, Shaikh IA, Shettar AK, Hoskeri JH, Kumbar V. Synthesis and characterization of silver nanoparticles from Rhizophora apiculata and studies on their wound healing, antioxidant, anti-inflammatory, and cytotoxic activity. Molecules. 2022; 27(19):6306. https://doi.org/10.3390/molecules27196306
42. Anandalakshmi K, Venugobal J, Ramasamy V. Characterization of silver nanoparticles by green synthesis method using Pedalium murex leaf extract and their antibacterial activity. Appl. Nanosci. 2016; 6: 399–408. https://doi.org/10.1007/s13204-015-0449-z
43. Willian N, Syukri S, Zulhadjri Z, Pardi H, Arief S. Marine plant mediated green synthesis of silver nanoparticles using mangrove Rhizophora stylosa: Effect of variable process and their antibacterial activity. F1000Research. 2022; 10:768. https://doi.org/10.12688/f1000research.54661.2
44. Acharya S, Patra DK, Pradhan C, Mohapatra PK. Anti-bacterial, anti-fungal and anti-oxidative properties of different extracts of Bruguiera gymnorrhiza L. (Mangrove). European Journal of Integrative Medicine. 2020; 36:101140. https://doi.org/10.1016/j.eujim.2020.101140.
45. Morones JR, Elechiguerra JL, Camacho A, Holt K, Kouri JB, Ramírez JT, Yacaman MJ. The bactericidal effect of silver nanoparticles. Nanotechnology. 2005; 16(10):2346-53. https://doi.org/10.1088/0957-4484/16/10/059
46. Rai M, Yadav A, Gade A. Silver nanoparticles as a new generation of antimicrobials. Biotechnology advances. 2009; 27(1):76-83. https://doi.org/10.1016/j.biotechadv.2008.09.002
47. Ahmed S, Ahmad M, Swami BL, Ikram S. Green synthesis of silver nanoparticles using Azadirachta indica aqueous leaf extract. Journal of radiation research and applied sciences. 2016; 9(1):1-7. https://doi.org/10.1016/j.jrras.2015.06.006
48. Sharma VK, Yngard RA, Lin Y. Silver nanoparticles: green synthesis and their antimicrobial activities. Advances in colloid and interface science. 2009; 145(1-2):83-96. https://doi.org/10.1016/j.cis.2008.09.002

49. Patil, S., Chandrasekaran, R., & Ramesh, T. Mangrove-mediated synthesis of silver nanoparticles and their biological applications. Marine Drugs. 2020; 18(3): 150.
50. Oke MA, Adebayo EA, Aina DA. Nitric oxide scavenging activity, total phenolic and flavonoid content of Persea americana fruit peel mediated silver, gold and alloy nanoparticles. Nano Plus Sci. Technol. Nanomater. 2021; 2:86-96. https://doi.org/10.48187/stnanomat.2021.2.006
51. Antony PT, Thiraviyam P, Kannan K, Ganapathy D, Sivaperumal P, Thangavelu L. Characterization and Biological Activities of Silver Nanoparticles from Mangrove Rhizophora Apiculata Extracts. Nanotechnology Perceptions. 2024; 20(S7):155-168. https://doi.org/10.62441/nano-ntp.v20iS7.12
52. Elangovan M, Rajesh K, Santhoshkumar M, Sathishkumar K, Bharathiraja N, Gnanasri M. Exploring the potential of agro-waste-mediated silver nanoparticles as antibacterial and antioxidant agents. Biomass Conversion and Biorefinery. 2024; 14(23):30591-30600. https://doi.org/10.1007/s13399-023-04945-9
53. Tundis R, Loizzo MR, Menichini F. Natural products as α-amylase and α-glucosidase inhibitors and their hypoglycaemic potential in the treatment of diabetes: an update. Mini reviews in medicinal chemistry. 2010; 10(4):315-31. https://doi.org/10.2174/138955710791331007
54. Kazeem MI, Adamson JO, Ogunwande IA. Modes of inhibition of α-amylase and α-glucosidase by aqueous extract of Morinda lucida Benth leaf. BioMed Research International. 2013; (1):527570. https://doi.org/10.1155/2013/527570
55. González-Garibay AS, Torres-González OR, Sánchez-Hernández IM, Padilla-Camberos E. Biosynthesized Silver Nanoparticles and Their Antidiabetic Potential. Pharmaceuticals. 2025 Sep 19;18(9):1412. https://doi.org/10.3390/ph18091412
56. Vishwakarma DK, Rana V, Singh V, & Kumar V. Green synthesis, characterization, and α-glucosidase/α-amylase inhibitory potential of silver nanoparticles using Costus igneus leaf extract. International Journal of Pharmacology and Clinical Research. 2025; 7(2): 281–289. https://www.doi.org/10.33545/26647613.2025.v7.i2d.120
57. Jini D, Sharmila S, Anitha A, Pandian M, Rajapaksha RM. In vitro and in silico studies of silver nanoparticles (AgNPs) from Allium sativum against diabetes. Scientific Reports. 2022; 12(1):22109. https://doi.org/10.1038/s41598-022-24818-x
58. Kumar S, Narwal S, Kumar V, Prakash O. α-glucosidase inhibitors from plants: A natural approach to treat diabetes. Pharmacognosy reviews. 2011; 5(9):19. https://doi.org/10.4103/0973-7847.79096
59. Bhavi SM, Mirji SK, Thokchom B, Singh SR, Maliger RB, Bhat SS, Joshi P, Harini BP, Yarajarla RB, Jadidi SA. Potential antidiabetic properties of Syzygium Cumini (L.) Skeels leaf extract-mediated silver nanoparticles. Austin J. Anal. Pharm. Chem. 2024; 11(1):1168.
60. Khodeer DM, Nasr AM, Swidan SA, Shabayek S, Khinkar RM, Aldurdunji MM, Ramadan MA, Badr JM. Characterization, antibacterial, antioxidant, antidiabetic, and anti-inflammatory activities of green synthesized silver nanoparticles using Phragmanthera austroarabica AG Mill and JA Nyberg extract. Frontiers in Microbiology. 2023; 13:1078061. https://doi.org/10.3389/fmicb.2022.1078061
61. Paul S, Sarkar I, Sarkar N, Bose A, Chakraborty M, Chakraborty A, Mukherjee S. Silver nanoparticles in diabetes mellitus: therapeutic potential and mechanistic insights. Bulletin of the National Research Centre. 2024 Mar 21;48(1):33. https://doi.org/10.1186/s42269-024-01182-6
62. Patel DK, Prasad SK, Kumar R, Hemalatha S. An overview on antidiabetic medicinal plants having insulin mimetic property. Asian Pacific journal of tropical biomedicine. 2012; 2(4):320-30. https://doi.org/10.1016/S2221-1691(12)60032-X